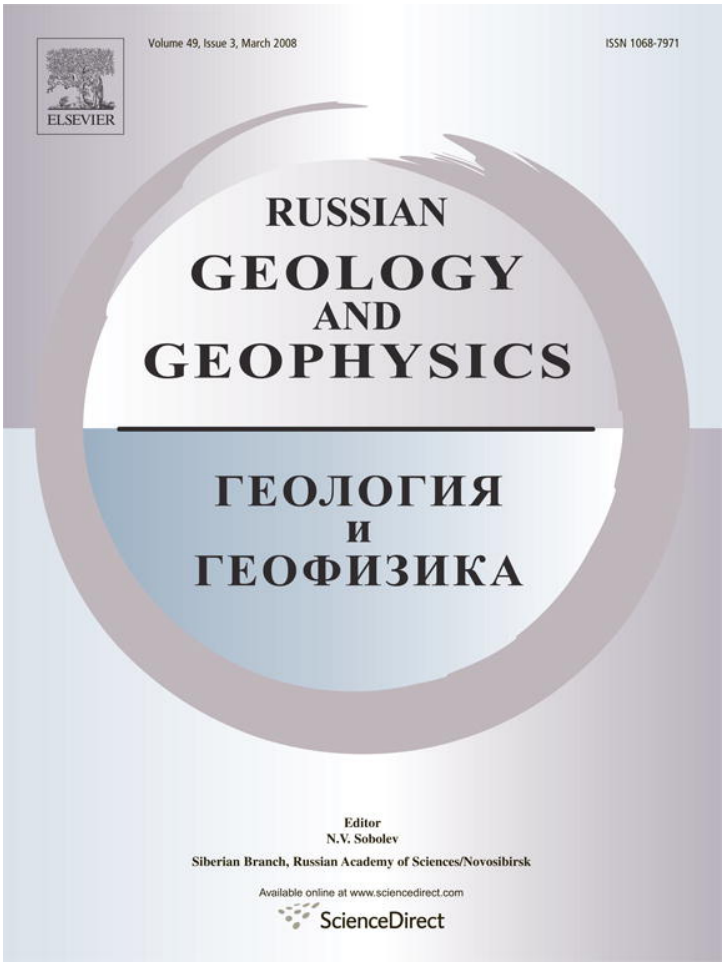

Available online at www.sciencedirect.com
ScienceDirect
Russian Geology and Geophysics 49 (2008) 187–196
RUSSIAN GEOLOGY AND GEOPHYSICS
www.elsevier.com/locate/rgg

Upper mantle structure beneath southern Siberia and Mongolia, from regional seismic tomography

I.Yu. Kulakov *

Institute of Petroleum Geology and Geophysics, Siberian Branch of the RAS, 3 prosp. Akad. Koptyuga, Novosibirsk, 630090, Russia

Received 26 January 2007; accepted 25 June 2007

Abstract

Tomographic inversion of ~130,000 *P* and ~11,000 *S* arrivals from 1045 events recorded by the world seismological network (ISC catalog data) has been applied to image the three-dimensional velocity structure of the upper mantle beneath the Baikal rift and Mongolia. The inversion-derived *P* and *S* velocity anomalies show a good agreement. At depths above 200 km, low-velocity zones occur along the contours of the high-velocity Siberian craton and in Mongolia and coincide with fields of Cenozoic volcanism. The deeper mantle appears quite homogeneous, with anomalies no greater than 0.5% and a single low-velocity feature beneath the Siberian craton. The tomographic image is poorly consistent with the hypothesis implying the existence of large mantle plumes under Mongolia which has been checked with synthetic tests. According to the tomography-based geodynamic model, volcanism in the East Sayan mountains may be induced by a hot plume rising from beneath the Siberian craton, but the source of volcanism in the area of Hangayn remains open to discussion.

Keywords: Seismic tomography; upper mantle; Baikal rift; southern Siberia; Mongolia

Introduction

There has recently been much discussion on plate interaction and mantle controls of neotectonic processes in the evolution of the Central Asian lithosphere. A detailed analysis of each factor for the case of southern Siberia can be found in (Dobretsov et al., 1996; Kuz'min et al., 2003; Laverov et al., 2006; Yarmolyuk and Kovalenko, 2003). The effect of mantle processes, however, cannot be properly estimated without comprehensive studies of the mantle structure.

Signature of the mantle control of neotectonics in southern Siberia and Mongolia appears in local Cenozoic volcanism (Logachev, 2005) which may originate from deep mantle sources (Aschepkov, 1991). The reported tomographic study aimed at detecting upper mantle convection or plume sources of the volcanism. The plumes, if there are any beneath Siberia and Mongolia, must be relatively small and tomographically irresolvable but one could expect to discover hot mantle zones as their implicit evidence. The objective was to image the three-dimensional velocity structure of the upper mantle to a depth of 670 km and to correlate the velocity anomalies to real structures in the Earth. Another objective was to assess the resolution power of the available observation system.

Historic background

Natural-source teleseismic tomography is among few geophysical tools of imaging the mantle. Tomographic scanning of mantle beneath Asia was first approached in the 1970s. First regional models in Russia appeared in (Alekseev et al., 1971; Gobarenko and Yanovskaya, 1983). Outside Russia, they were P_n and S_n (Barazangi, Ni, 1982; Ni and Barazangi, 1983) and surface-wave (Bourjot and Romanowicz, 1992; Brandon and Romanowicz, 1986; Pines et al., 1980) tomographic models.

The mantle structure of Asia has been a subject of several recent publications. Wu et al. (1994, 1997) studied the distribution of Rayleigh-wave group velocities beneath Central Asia. Their results were extended and updated in (Huang et al., 2003; Maceira et al., 2005; Ritzwoller and Levshin, 1998; Yanovskaya and Kozhevnikov, 2000). Friederich (2003) modeled the *S* velocity structure of the East Asian mantle to a depth of 700 km using joint inversion of shear and surface waveforms. Yet, the high- and low-velocity zones in the cited models were too large to be matched to specific geological

* Corresponding author.
E-mail address: ivan2art@gmail.com (I.Yu. Kulakov)

1068-7971/$ - see front matter © 2008, IGM, Siberian Branch of the RAS. Published by Elsevier B.V. All rights reserved.
doi:10.1016/j.rgg.2007.06.016

structures. A better resolution and consistency was achieved due to surface-wave tomography by Villasenor et al. (2001) and Ritzwoller et al. (2002) with P_n and S_n phases. Of all cited studies, the global tomography by Bijwaard et al. (1998) appears to be the most reliable and is used below as a check of our model. The three latter models are based on different data and algorithms (Bijwaard et al., 1998; Ritzwoller et al., 2002; Villasenor et al., 2001) but show good agreement, which confirms their validity.

It is reasonable to explore the deep structure of Central Asia, where seismic activity is high but the available regional networks are rather scarce, using the Inverse Tomographic Scheme (ITS) as reported in (Koulakov, 1998; Koulakov et al., 2002; 2003). The previous ITS versions, however, did not give much attention to earthquake location and testing. The improved ITS version (Koulakov and Sobolev, 2006) used in this study provided a more faithful image of the upper mantle.

Tectonic and volcanic activity in southern Siberia and Mongolia

Southern Siberia and Mongolia are located in the north of the Alpine-Himalayan orogen. One can see in an elevation map (Fig. 1) how mountain terrains patched with stable blocks abut against the weakly deformed areas of the West Siberian Plate and Siberian craton. The Baikal rift system, one of the world's largest continental rifts, is a major tectonic unit of the region. It stretches as an over 1500 km chain of basins and ranges along the boundary between the Siberian craton and the Amur-Mongolia block. The largest rift basin, about 680 km long, is occupied by Lake Baikal and delineates the southeastern craton margin. The Baikal basin comprises three subbasins (South, Central, and North Baikal) that differ in age and activity patterns.

The flank of the rift system southwest of Lake Baikal consists of the W-E Tunka basin, the nearest to Baikal, and three equally spaced N-S basins (Hövsgöl, Darhat, and Busiyngol). Note that seismic activity is the lowest in the largest Hövsgöl basin but is Siberia's highest in the small Busiyngol basin (Emanov et al., 2001). In the south, the rift system is truncated by the W-E Bulnayn strike-slip fault, a regional shear zone that extends for thousands of kilometers in Mongolia.

The northeastern rift flank is a series of numerous small and large basins (Barguzin, Upper Angara, Tsipa, and Muya basins are the largest) with mountains between them.

The Baikal system generally experiences typical rift extension (San'kov et al., 1999) evidenced by abundant normal faults along the basin borders (Doser, 1991; Logachev, 2005; Zorin and Cordell, 1991) and high seismicity (Déverchère et al., 2001; Radziminovitch et al., 2003, 2005) with at least thirteen $M > 6.5$ events for the past 280 years (Doser, 1991), and especially by extensional earthquake mechanisms (Lesne et al., 2000; Petit et al., 1996). Rift-orthogonal extension at 4–5 mm/yr was also inferred from GPS data (Calais et al., 2003; Vergnolle et al., 2003).

Rifting in the Baikal system began about 30 Myr ago, when the India-Eurasia collision was in its most active stage. This fact is a critical argument for the idea that the collision and the ensuing plate motion triggered the Baikal rifting (passive rifting model).

On the other hand, the local presence of Cenozoic volcanic fields in the rift, with a total of 6000 km^3 erupted lavas (Logachev et al., 1996; Logachev, 2005), indicates that mantle processes played a certain role. Most of eruptions occurred in the Sayan-Khamar-Daban area while the activity in two other fields (Udokan and Vitim) released 800–1000 km^3 of lavas and pyroclastics. Surprisingly, no traces of young volcanism have been found in the largest rift basin of Lake Baikal: the youngest sporadic igneous rocks within it are at least 52 Ma (Eskin et al., 1978; Logachev, 2005). The three volcanic fields lie mainly off the rift basins. In the southwestern rift flank, there is some occurrence of volcanism in the Tunka basin (Sayan-Khamar-Daban area) but almost no volcanics in the Hövsgöl, Darhat, and Busiyngol basins in Mongolia (Yarmolyuk et al., 1990). Another paradox is quite a low heat flow in the East Sayan (Duchkov and Sokolova, 1974; Lysak, 1988), much lower than one would expect in an area of active volcanism.

It is relevant to mention small fields of Cenozoic magmatism in Mongolia, in the northeastern Hangayn plateau (Fig. 1), which were attributed to branches of a single hotspot in the Sayan-Khamar-Daban area (Yarmolyuk et al., 1990, 1995). This hypothesis is supported by similar compositions and ages of magmas.

According to their structure and composition as detailed in (Rasskazov, 1993), Cenozoic lavas in the Baikal rift system were derived from more or less similar sources at depths of 50 to 150 km. On the other hand, the chemistry of mantle xenoliths (Ashchepkov et al., 1996; Dobretsov and Ashchepkov, 1991; Kuz'min et al., 2003; Yarmolyuk and Kovalenko, 2003) is consistent with their origin at greater mantle depths. Magmatism in the Baikal rift system apparently acted in cyclic pulses with peaks at approximately 60, 30 and 10 Ma separated by 10–15 Myr long lulls (Rasskazov et al., 1990).

Volcanism is the youngest in the East Sayan, where it shows a northwestern migration trend presumably associated with the motion of the Eurasian plate at 0.9 cm/yr (Rasskazov, 1994). Rasskazov (1994) explained the location of volcanism along the craton edge by the presence of a mantle plume impinged on and spread beneath the lithospheric base.

ITS algorithm and data

The three-dimensional velocity mantle structure has been studied using the inverse tomographic scheme (ITS). Originally ITS was suggested as an alternative to the classical (forward) teleseismic scheme for areas where the seismological networks are too scarce to allow reliable tomographic imaging. The basic ITS requirement is the availability of a sufficient number of earthquakes in the scanned region

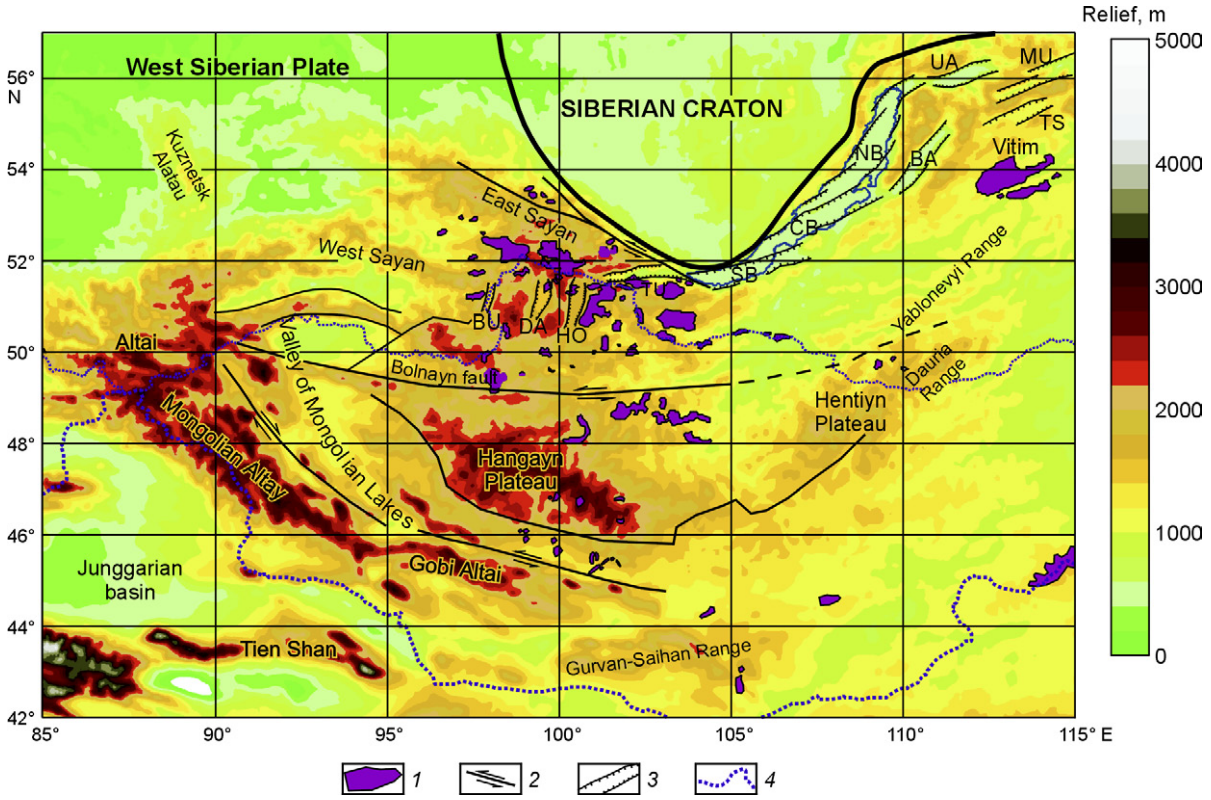

Fig. 1. Elevation and generalized tectonics of study region, after (Zorin et al., 2003), etc. *1* — fields of Cenozoic volcanism; *2*, *3* — strike-slip (*2*) and normal (*3*) faults; *4* — national frontiers. Abbreviations stand for names of rift basins, keyed as: BU — Busiyngol, DA — Darhat, HO — Hövsgöl, TU — Tunka, SB — South Baikal, CB — Central Baikal, NB — North Baikal, BA — Barguzin, UA — Upper Angara, MU — Muya, TS — Tsipa.

recorded by the global network. The earlier ITS versions (Koulakov, 1998; Koulakov et al., 2002, 2003) employed teleseismic rays only and missed the earthquake relocation procedure. In the more recent versions (Koulakov et al., 2006), processed are all rays available in catalogs: short distances are used for earthquake location and teleseismic distances for deep structure imaging.

The ITS algorithm is designed for inversion of *P* and *S* arrivals from earthquakes inside a study area registered in international earthquake catalogs to obtain the three-dimensional *P* and *S* velocity structure and earthquake location. Regional tomographic inversion is performed in a number of circular areas with user-specified coordinates and the radii normally comparable to the scanned depths. The upper mantle is imaged using circles of 1200–1600 km in diameter. Inversion of earthquake data selected from a circle is performed for several parameterization grids oriented in different directions. An area larger than a circle can be studied by stacking inversion results for several overlap circles. The ITS algorithm is based on the linearized approach in which velocity anomalies are computed in a single iteration from rays in the reference 1D model. The reason is that obtaining stable results with the noisy ISC data requires a great amount of processing. The use of nonlinear approaches (especially, 3D ray tracing) makes the problem insurmountable with the available computing facilities. Linearized inversion is quite workable because the minor velocity variations in the upper mantle (no more than 5%) cannot cause much change to the ray paths and, correspondingly, much errors. For more details of the algorithm see (Koulakov and Sobolev, 2006).

Data have been borrowed from the ISC catalog (2001) which offers information on earthquakes for the period from 1964 through 2001 and arrivals to all available stations of the world network (about 7000).

In this study, inversion was applied to about 130,000 *P* and 11,000 *S* arrivals from 1045 events in southern Siberia and Mongolia. See Fig. 2 for the layout of the observation system, with the positions of earthquakes and stations in two scales in the equidistant projection. The greatest contribution to the system of teleseismic rays was from stations in Europe and America which ensured scanning in the NW and NNE directions. Many of regional rays arrived from stations in China, i.e., from the south. Regional rays were mainly used for earthquake relocation and for improving the vertical resolution of the image. Inversion was performed in five separate circles of 7° radius each (Fig. 3, *a*, *b*, upper sections).

All earthquakes from the ISC catalog were relocated using the ITS algorithms, with culling out over 15% outliers.

Inversion of real data

Inversion of arrivals reduced the RMS error in *P*- and *S*-wave data for 35 to 45% and 30 to 40%, respectively, in

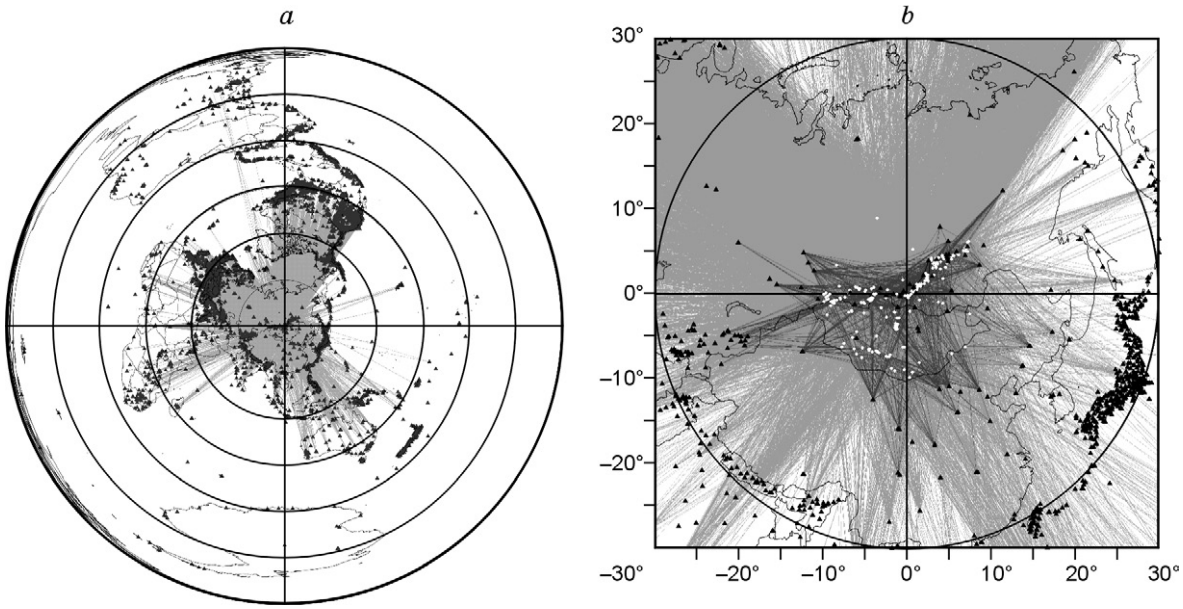

Fig. 2. Layout of observation system. *a* — equidistant projection centered on study area. Circles are spaced at 30° of epicentral distance relative to 103° E, 52° N. Triangles are stations of world seismological network. *b* — enlarged fragment corresponding to epicentral distance of 30°. White dots are earthquakes in study region. Dark lines are rays with epicentral distances less than 20° that travel only in upper mantle.

different circles. The relatively low error reduction was due to high noise in the data and, on the other hand, to rather low intensities of velocity anomalies (see below). The inversion results are shown in horizontal sections in Fig. 3, *a*, *b* and in a vertical cross section (Fig. 4). There is obvious correlation between the *P* and *S* velocity patterns which is implicit evidence for the reliability of the models. Most intense low-velocity zones occur at depths of 50 and 100 km along the southern craton periphery. The velocity anomalies are especially prominent in the East Sayan, in the area of Cenozoic volcanism. The Siberian craton shows up as a high-velocity zone to at least 200–250 km deep.

Generally, velocity contrasts are more or less significant (3–5%) above 200 km while the lower mantle appears rather homogeneous with anomalies less than one percent below 300 km.

Note that inversion-derived velocity anomalies are commonly lower than in the reality (see the synthetic tests below). This uncertainty is an intrinsic drawback of the method arising in almost any tomographic study. In our case, the magnitude of anomalies may be underestimated for a factor of 1.5–2.

The validity of the ITS-derived mantle velocity structure can be checked against other tomographic models (Bijwaard et al., 1998). Bijwaard's model (Fig. 5) appears to be one of most detailed and robust ever obtained. The two models share the same velocity pattern in the upper sections and a low magnitude of lower mantle velocity anomalies (under 1%), though the latter are of slightly different configurations. This difference means that the correct geometry of high- or low-velocity zones at lower mantle depths is difficult to resolve because of a low signal/noise ratio. The only feature recognizable more or less reliably is a low-velocity zone beneath the Siberian craton.

The ITS-derived upper mantle velocity structure is also compatible with inversion of P_g, S_g, P_n, and S_n data from the Baikal regional seismological network (Yakovlev et al., 2007).

Synthetic tests

Chequerboard test. The resolution power of the observation system was checked by the chequerboard synthetic test (Fig. 6). The cell sizes (150 and 250 km for *P* and *S* models, respectively) were less than the characteristic size of features obtained in inversion of real data. Synthetic residuals were computed from rays used in the real observation system and added with 0.4 s random noise; 10% data were intentionally spoiled by increasing the noise by a factor of 10. The multiplied noise simulated outliers in a real data catalog. After the synthetic travel times had been computed, the user "forgot" the locations of events and, like in the real case, launched the inversion procedure with earthquake location. The processing procedure for synthetic data was the same as for the real data. Thus, the test was a faithful model of the real conditions. The synthetic test would inevitably highlight any significant uncertainty (due to noise or too long distances from the stations) in inversion-derived source parameters.

The inversion of synthetic data (Fig. 6) validated the ITS results for the greatest part of the territory at all depth intervals. The best resolution was at medium depths between 200 and 300 km while the features below 300 km looked diffuse and 1.5–2 times less intense than in the reality.

Checking the hypothesis of plumes beneath Mongolia. Zorin et al. (2003; Zorin and Turutanov, 2005) hypothesized the presence of plumes in the upper mantle under the Baikal rift and Mongolia proceeding from smoothed gravity data. The

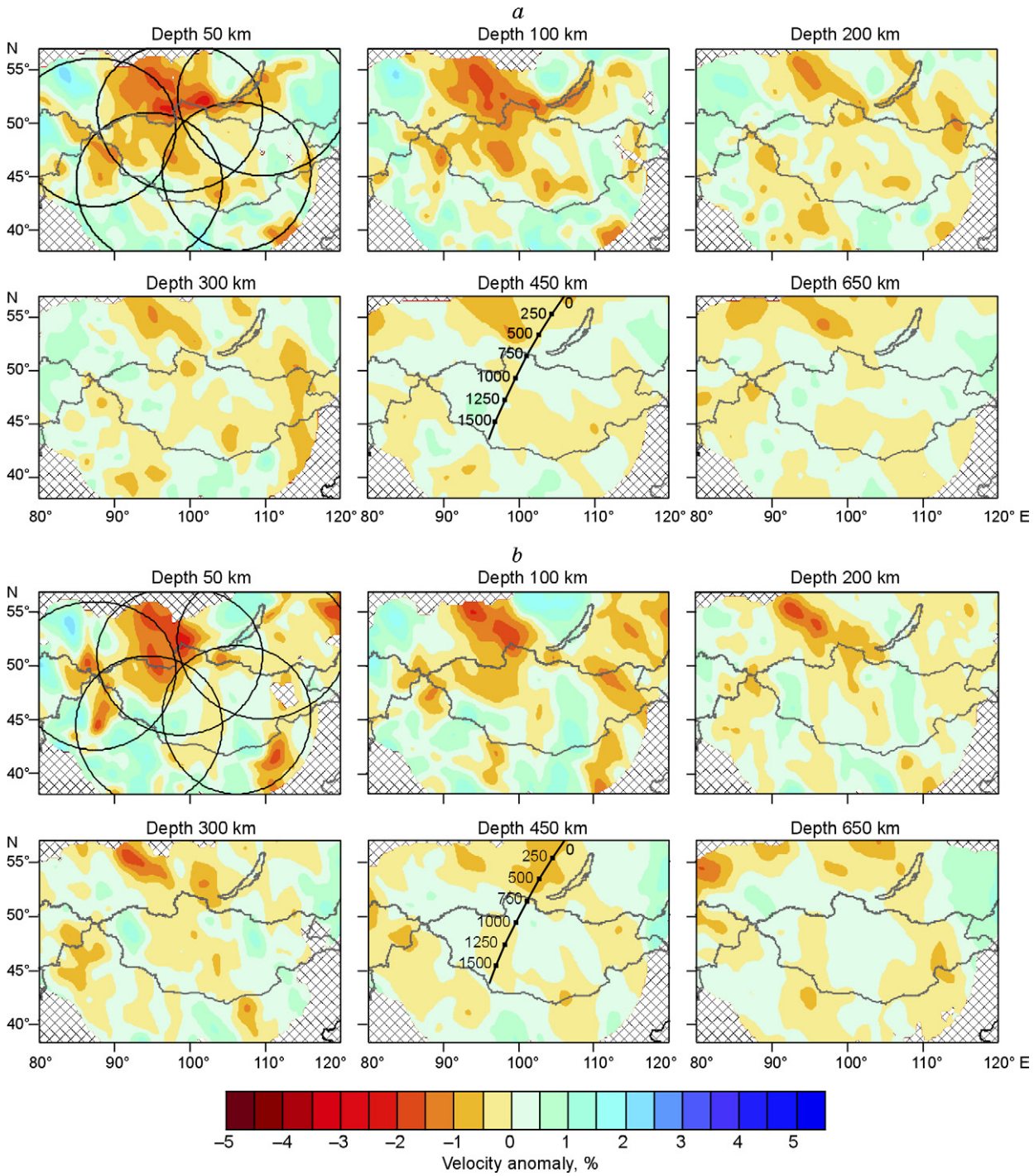

Fig. 3. *P* (*a*) and *S* (*b*) velocity anomalies obtained by ITS inversion of real data from southern Siberia and Mongolia. Circles in upper sections contour areas of independent ITS inversion.

gravity field was consistent with the effect from five plumes, and their position fitted the pattern of Cenozoic volcanism. The model appears quite realistic, the observed and computed gravity fields being in good agreement.

However, the plume model contradicts the tomographic model showing no large features at depths below 300 km over the greatest part of Mongolia and southern Siberia. The deep mantle velocity structure bears no signature of the five plumes (Zorin et al. 2003); the only low-velocity zone that can be taken for a plume trace occurs beneath the Siberian craton.

The reason might be in a low horizontal resolution of tomography. This guess was checked with a test (Fig. 7) in which velocity anomalies in the upper mantle above 150 km were specified following the real inverted data and the reference model for the depths between 150 and 700 km consisted of five plumes located as in (Zorin et al., 2003). The plume sizes in the *P* and *S* models were ~200 km and the related velocity contrast was 3%. As in the case of the chequerboard test, 0.4 s random noise was added to synthetic data and 10% outliers were generated additionally with a 10

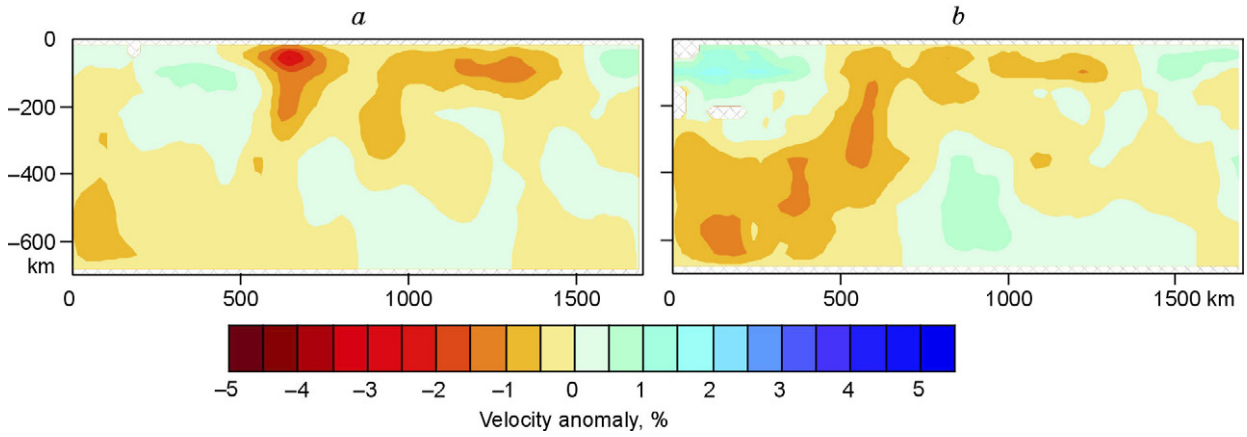

Fig. 4. *P* (*a*) and *S* (*b*) velocity anomalies obtained by ITS inversion in vertical section. For position of profile see sections corresponding to depth of 450 km in Fig. 3, *a*, *b*.

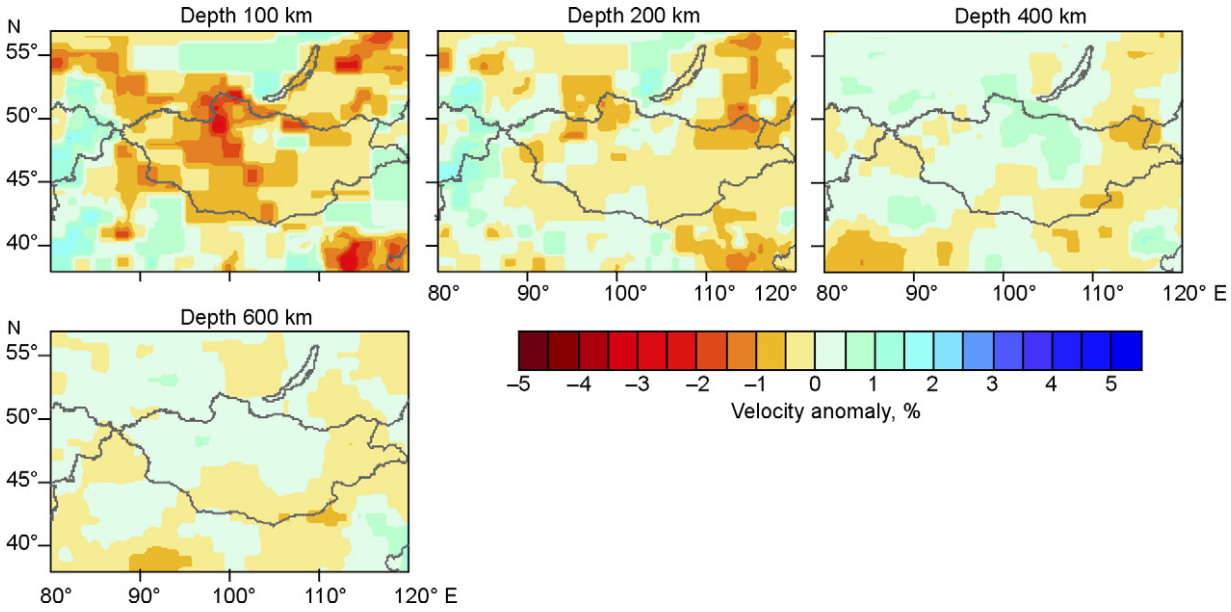

Fig. 5. *P*-wave velocity anomalies beneath southern Siberia and Mongolia in four horizontal sections according to global tomography of Bijwaard et al. (1998).

times greater error, which approximately corresponded to the real data processing conditions.

Inversion of the synthetic data showed a satisfactory resolution power of the system for reconstructing main velocity features in the *P* and *S* models at depths above 150 km. Plumes in the lower layer appeared only in the *P* model; some weak plume traces in the *S* model were about the noise level. At the same time, the fact that the plumes are recognizable in the synthetic *P* model and remain undetectable in the real data inversion disproves the existence of plumes with such a geometry beneath Mongolia and southern Siberia.

One may hypothesize that the plumes beneath Siberia and Mongolia are smaller than in Zorin's model and are less than 100 m thick. Features of this size elude detection by the tomographic method, possibly because of low resolution, which was checked in the synthetic tests, but especially because of the nonlinearity effect. A ray in 3D ray tracing tends to round small low-velocity zones to minimize the travel time, according to the Fermat principle. As a result, the plume-related residuals are much less than in linearized inversion in which the ray geometry is independent of velocity variations. The resulting inversion obviously gives a more diffuse image than the linearized approach. Unfortunately, the current ITS version failed to include the 3D ray tracing procedure, but it is clear qualitatively that the nonlinearity effect would make irresolvable the plumes less than 100 km.

On the other hand, a real ray is rather a banana-like Fresnel zone than a line, and its thickness depends on the frequency of the seismic signal. Adaptation of the imaging procedure with regard to this fact can help detecting more subtle features than the simple ray tomography (Montelli et al., 2004). Therefore, if the plumes under Siberia and Mongolia do exist

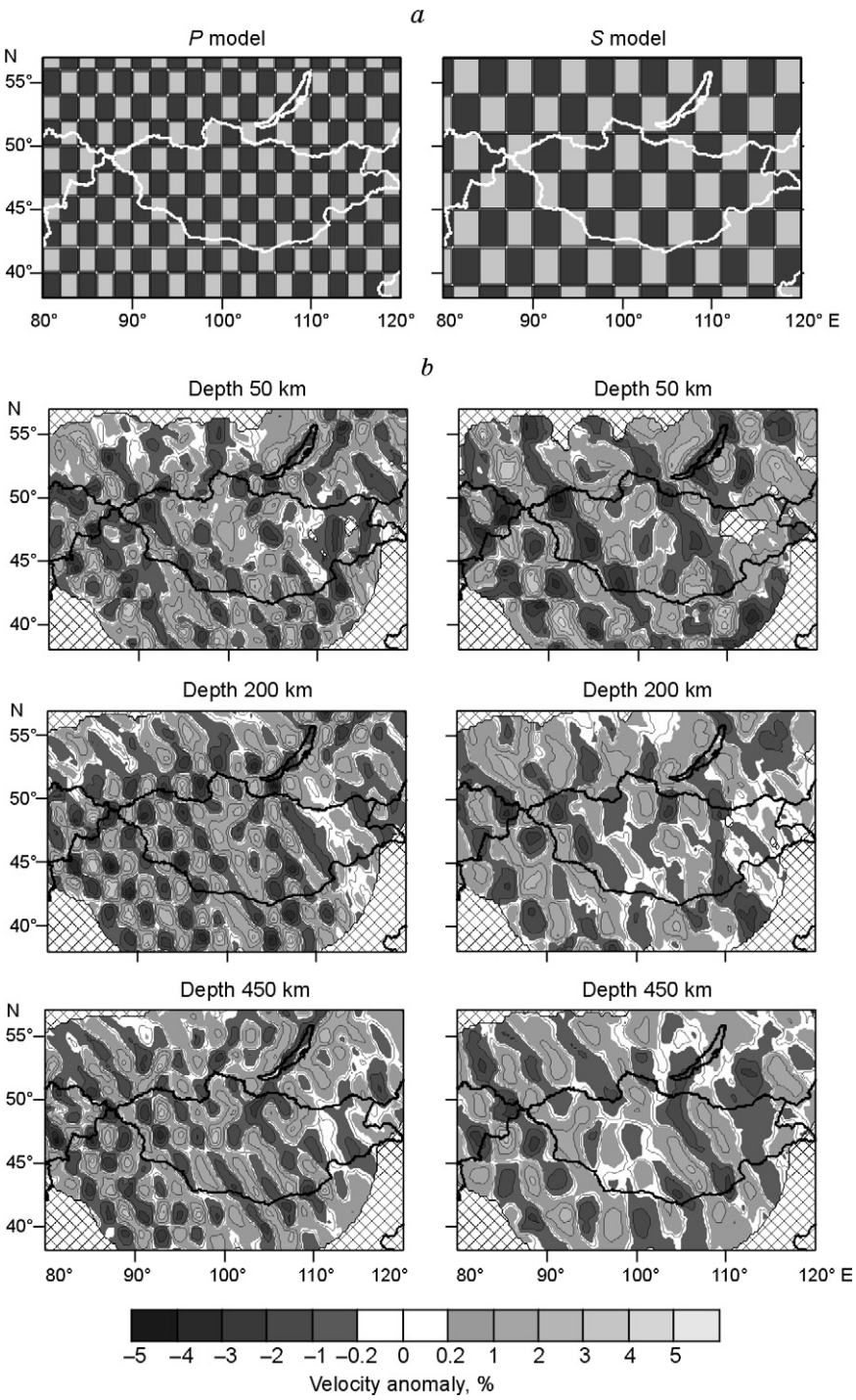

Fig. 6. Chequerboard test for *P* and *S* models. *a* — initial models, 0.4 s noise; *b* — inversion results.

but elude tomographic imaging, they must be too small (<100–150 km in diameter) and/or young. Then, they would be unable to produce a tomographically recognizable large hot zone around them. A plume four times smaller than in Zorin's model will cause a density deficit of 80 instead of 20 kg/m^3 (quite an admissible value for a plume) but the gravity effect will be the same as in (Zorin et al., 2003). However, such a small plume is beyond the resolution power of tomographic imaging.

Geodynamic model

The ITS results were used to develop a geodynamic model (Fig. 8) with reference to the *S*-velocity pattern which is more sensitive to temperature variations in the mantle. The model supposes the existence of a plume beneath the Siberian craton. It is apparently not so weak because it produces a large subcratonic low-velocity zone presumably corresponding to hot mantle around the plume. The plume, if its size is 100 km

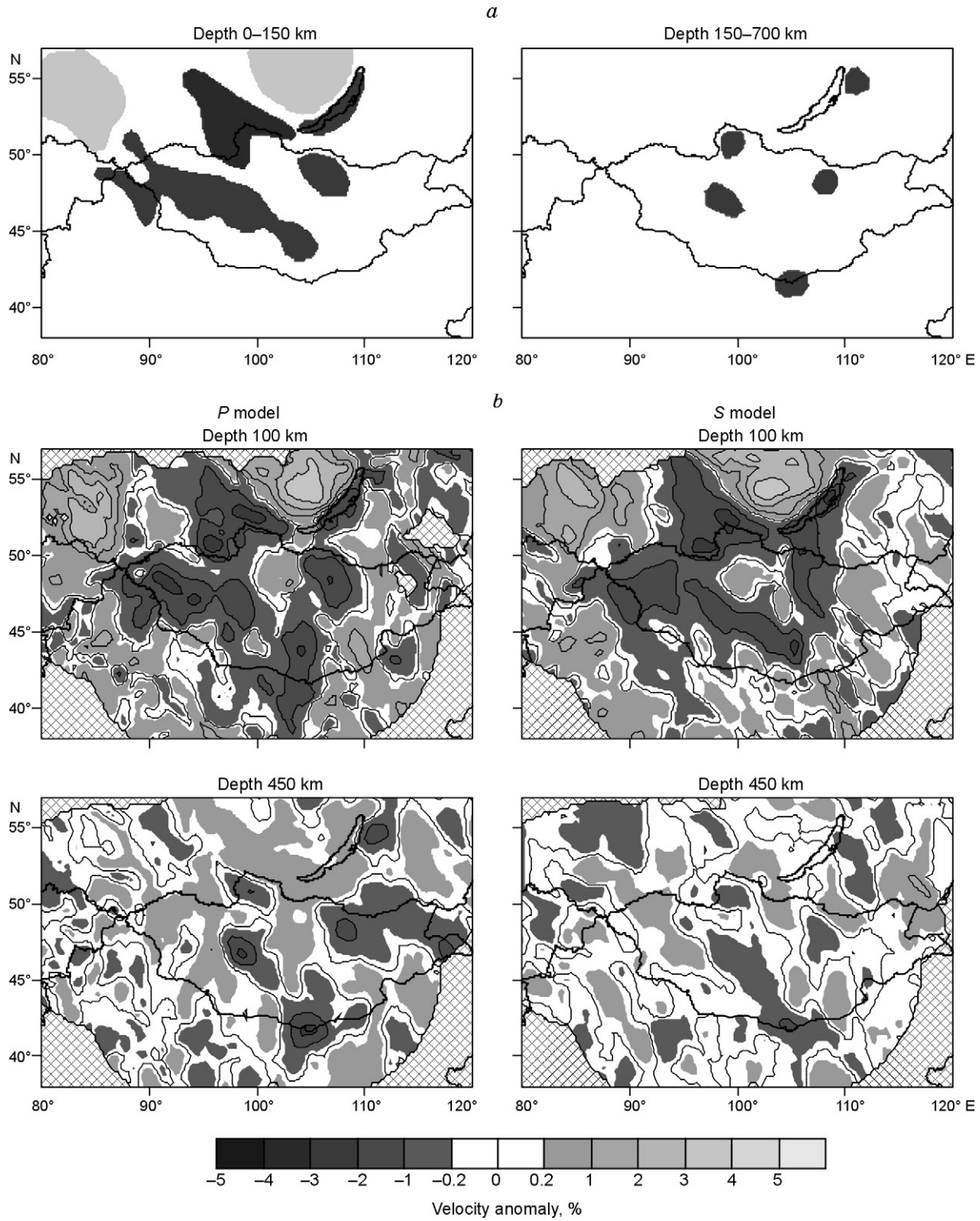

Fig. 7. Inversion of synthetic data simulating real conditions. *a* — initial velocity anomalies. Anomalies at depths 0–150 km are specified according to inversion of real data; anomalies at 150–700 km simulate plumes according to Zorin et al. (2003); *b* — inversion results for *P* and *S* models.

or less, is hardly detectable by seismic methods. The effect of the plume can be that hot material stacks at the craton base and, having reached some critical volume, moves toward the southwestern craton edge. The discontinuous movement of hot mantle material beneath the craton can account for the cyclicity of volcanism in the East Sayan (Rasskazov et al., 1990). The old age of volcanism of at least 70 Ma (Rasskazov et al., 1990) is evidence for the stability of the subcratonic plume position.

According to mathematical modeling (Tychkov et al., 1998, 1999), the location of a plume under the thick cratonic lithosphere may be associated with mantle heating because of

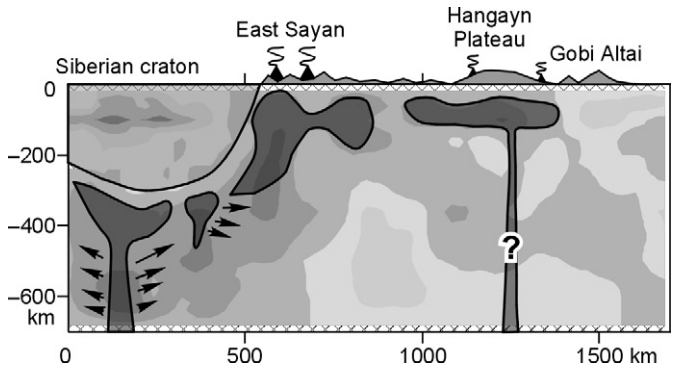

Fig. 8. ITS-based geodynamic model. Background is *S*-wave velocity pattern of Fig. 4, *b*. Hypothesized plumes are in dark. Arrows show possible directions of heat transport.

low heat transport from beneath the craton. The same setting occurs in the area of the Kenyan plume (Koulakov, 2007).

There might exist another plume (Fig. 8) beneath the Hangyan plateau, but it remains uncertain. Its location in the suggested model was selected following Zorin et al. (2003) but it did not show up in the tomographic image, possibly because of its small size and/or young age. Or, the Hangayn plume may have moved relative to the surface as a result of rotation of the Mongolian microplate and arrived at its current position only recently. Both hypotheses (plume's small size and relative motion) are consistent with independent modeling results of Dobretsov et al. (2001). Then, the plume would fail to heat large amounts of surrounding material to appear in the tomographic image. There are several arguments to support the existence of the Hangayn plume. First, it is the occurrence of Cenozoic lavas of evidently deep origin in the area of Hangayn. The lavas must come from a local source because arrival of the erupted material from beneath the Siberian plate hardly can be explained by any feasible mechanism that would provide a southward lateral transport for 700–800 km. Second, there is a gravity low around the Hangayn in the long-wave component of the gravity field which may be produced by a plume (Zorin et al., 2003).

Conclusions

Thus, the tomographic model fails to recognize traces of mantle plumes beneath Mongolia. Teleseismic tomography can reliably resolve features more than 200 km thick whereas smaller features are irresolvable for the basic limitations of the ray theory. The limitations are mainly due to the 3D geometry of the ray path and to the finite size of the Fresnel zone for the low frequency of the seismic signal. Plumes of the expected size (<100 km) would elude detection in the teleseismic method even with an orders of magnitude larger data collection.

The only possible way to image small features in the mantle is deploying campaign seismic networks immediately over the hypothesized plume. In this case, the use of teleseismic schemes and/or the receiver function method can provide quantitative estimates of the plume size and intensity. Successful plume detection experiments were performed in Europe, in the Central Massif (France) and in the Eifel volcanic field (Germany). A similar study in Mongolia would shed light on the mantle control of the ongoing tectonic movements in Central Asia.

References

Alekseev, A.S., Lavrentiev, M.M., Mukhometov, R.G., Neresov, N.L., Romanov, V.G., 1971. Numerical methods of investigation of the Earth's upper mantle structure, in: Mathematical Problems of Geophysics [in Russian]. Computer Center SB AS USSR, Novosibirsk, Issue 2, pp. 143–165.

Ashchepkov, I.V., Litasov, Yu.D., Litasov, K.D., 1996. Xenoliths of garnet lherzolites from metanephelinites, the Khentei Ridge (Southern Transbaikalia): evidence for the uplift of mantle diapir. Geologiya i Geofizika (Russian Geology and Geophysics) 37 (1), 130–147 (121–137).

Ashchepkov, I.V., 1991. Mantle Xenoliths of the Baikal Rift [in Russian]. Nauka, Novosibirsk.

Barazangi, M., Ni, J., 1982. Velocities and propagation characteristics of P_n and S_n beneath the Himalayan arc and Tibetan Plateau: Possible evidence for underthrusting of Indian continental lithosphere beneath Tibet. Geology 10, 179–185.

Bijwaard, H., Spakman, W., Engdahl, E.R., 1988. Closing the gap between regional and global travel time tomography. J. Geophys. Res. 103, 30,055–30,078,

Bourjot, L., Romanowicz, B., 1992. Crust and upper-mantle tomography in Tibet using surface waves. Geophys. Res. Lett. 19, 881–884.

Brandon, C, Romanowicz, B., 1986. A "no-lid" zone in the Central Chang-Thang platform of Tibet: Evidence from pure path phase velocity measurements of long-period Rayleigh waves. J. Geophys. Res. 91, 6547–6564.

Calais, E., Vergnolle, M., San'kov, V., Lukhnev, A., Miroshnitchenko, A., Amarjargal, S., Déverchère, J., 2003. GPS measurements of crustal deformation in the Baikal-Mongolia area, 1994–2002. J. Geophys. Res. 108 (B10), doi:10.1029/2002JB002373.

Déverchère, J., Petit, C, Gileva, N., Radziminovitch, N., Melnikova, V., San'kov, V., 2001. Depth distribution of earthquakes in the Baikal rift system and its implications for the rheology of the lithosphere. Geophys. J. Intern. 146(3), 714–730.

Dobretsov, N.L., Ashchepkov, I.V., 1991. Composition and evolution of upper mantle in rift zones (by example of BRZ). Geologiya i Geofizika (Soviet Geology and Geophysics) 32 (1), 5–13 (1–8).

Dobretsov, N.L., Buslov, M.M., Delvaux, D., Berzin, N.A., Ermikov, V.D., 1996. Mezo- and Cenozoic tectonics of the Central Asian mountain belt: effect of lithospheric plate interaction and mantle plume. Intern. Geol. Rev. 38, 430–466.

Dobretsov, N.L., Kirdyashkin, A.G., Kirdyashkin, A.A., 2001. Deep Geodynamics [in Russian]. Izd. SO RAN, filial "Geo", Novosibirsk.

Doser, D., 1991. Faulting within the western Baikal rift as characterized by earthquake studies. Tectonophysics 196, 87–107.

Duchkov, A.D., Sokolova, L.S., 1974. Geothermal Studies in Siberia [in Russian]. Nauka, Novosibirsk.

Emanov, A.A., Emanov, A.F., Seleznev, B.C., Filina, A.G., 1978. Approaches to space-time relationships in seismicity of the Altai-Sayan folded area, in: Problems of Regional Geophysics [in Russian]. Tipografiya Sibiri, Novosibirsk, pp. 65–67.

Eskin, A.S., Bukharov, A.A., Zorin, Yu.A., 1978. Cenozoic magmatism of Lake Baikal. Dokl. Akad. Nauk SSSR 239 (4), 926–929.

Friederich, W., 2003. The S-velocity structure of the East Asian mantle from inversion of shear and surface waveforms. Geophys. J. Intern. 153, 88–102.

Gobarenko, B.C., Yanovskaya, T.B., 1983. The study of the structure of horizontal heterogeneities in the upper mantle of the Altai-Sayan zone. Izv. AN SSSR, Ser. Fizika Zemli 4, 21–35.

Huang, Z., Su, W., Peng, Y., Zheng, Y., Li, H., 2003. Rayleigh wave tomography of China and adjacent regions. J. Geophys. Res. 108(B2), 2073, doi:10.1029/2001JB001696.

International Seismological Centre, Bulletin Disks 1-9 [CD-ROM], 2001. Internatl. Seis. Cent., Thatcham, United Kingdom.

Koulakov, I.Yu., Sobolev, S.V., 2006. A tomographic image of Indian lithosphere break-off beneath the Pamir-Hindukush Region. Geophys. J. Intern. 164, 425–440.

Koulakov, I.Yu., 1998. 3D tomographic structure of the upper mantle beneath the central part of Eurasian continent. Geophys. J. Intern. 133 (2), 467–489.

Koulakov, I., Tychkov, S., Bushenkova, N., Vasilevskiy, A., 2002. Structure and dynamics of the upper mantle beneath the Alpine-Himalayan orogenic belt, from teleseismic tomography. Tectonophysics 358, 77–96.

Koulakov, I.Yu., 2007. Structure of the Afar and Tanzania plumes based on regional tomography using ISC data. Dokl. Earth Sci. 417 (8), 1287–1292.

Kuz'min, M.I., Al'mukhamedov, A.I., Yarmolyuk, V.V., Kravchinsky, V.A., 2003. Rift and within-plate magmatism in the context of hot and cold mantle fields. Geologiya i Geofizika (Russian Geology and Geophysics) 44 (12), 1270–1279 (1226–1234).

Laverov, N.P., Kovalenko, V.I., Yarmolyuk, V.V., Bogatikov, O.A., Akinin, V.V., Gurbanov, A.G., Evdokimov, A.N., Kudryashova, E.A., Pevzner, M.M., Ponomareva, V.V., Sakhno, V.G., 2006. Recent volcanism in Northern Eurasia: Regionalization and formation settings. Dokl. Eath Sci. 410 (7), 1048.

Lesne, O., Calais, E., Déverchère, J., Hassani, R., Chery, J., 2000. Dynamics of intracontinental extension in the North Baikal Rift from two-dimensional numerical deformation modeling. J. Geophys. Res. 105, 21727–21744.

Logachev, N.A., 2005. History and geodynamics of the Baikal rift, in: Goldin, S.V., Mazukabzov, A.M., Seleznev, B.C. (Eds.), Actual Problems of Modern Geodynamics of Asia [in Russian]. Izd. SO RAN, Novosibirsk, pp. 9–32.

Logachev, N.A., Rasskazov, S.V., Ivanov, A.V., Levi, K.G., Bukharov, A.A., Kashik, S.A., Sherman, S.I., 1996. Cenozoic rifting in continental lithosphere, in: Logachev, N.A. (Ed.), Lithosphere of Central Asia [in Russian], Nauka, Novosibirsk, pp. 57–80.

Lysak, S.V., 1988. Heat Flow of Continental Rift Zones [in Russian]. Nauka, Novosibirsk.

Maceira, M., Taylor, S.R., Amnion, C.J., Yang, X., Velasco, A.A., 2005. High-resolution Rayleigh wave slowness tomography of central Asia. J. Geophys. Res. 110, B06304, doi:10.1029/2004JB003429.

Montelli, R., Nolet, G., Dahlen, G.A., Masters, G., Engdahl, E.R., Hung, S.-H., 2004. Finite-frequency tomography reveals a variety of plumes in the mantle. Science 303, 338–343.

Ni, J., Barazangi, M., 1983. High-frequency seismic wave propagation beneath the Indian Shield, Himalayan Arc, Tibetan Plateau and surrounding regions: high uppermost mantle velocities and efficient S_n propagation beneath Tibet. Geophys. J. R. Astr. Soc. 72, 665–689.

Petit, S, Déverchère, J., Houdry, F., San'kov, V., Melnikova, V., Delvaux, D., 1996. Present-day stress field changes along the Baikal rift and tectonic implications. Tectonics 15, 1171–1191.

Pines, I., Teng, T.-L., Rosenthal, R., Alexander, S., 1980. A surface wave dispersion study of the crustal and upper mantle structure of China. J. Geophys. Res. 85, 3829–3844.

Radziminovich, N.A., Balyshev, C.O., Golubev, V.A., 2003. Earthquake focal depths and crustal strength in the Baikal rift. Geologiya i Geofizika (Russian Geology and Geophysics) 44 (11), 1216–1225 (1175–1183).

Radziminovitch, N.A., Déverchère, J., Melnikova, V., San'kov, V.A., Giljova, N., 2005. The 1999 Mw 6.0 earthquake sequence in the Southern Baikal rift, Asia, and its seismotectonic implications. Geophys. J. Intern. 161, 387–400.

Rasskazov, S.V., 1993. Magmatism of the Baikal Rift System [in Russian]. Nauka, Novosibirsk.

Rasskazov, S.V., 1994. Comparison of volcanism and Late Cenozoic structures of hot spots in Yellowstone and Eastern Sayan. Geologiya i Geofizika (Russian Geology and Geophysics) 35 (10), 67–75 (54–60).

Rasskazov, S.V., Batymurzaev, A.S, Magomedov, Sh.A., 1990. Cenozoic volcanism cycles of the southwestern Baikal region. Geologiya i Geofizika (Soviet Geology and Geophysics) 31(6), 64–72 (58–64).

Ritzwoller, M.H., Levshin, A.L., 1998. Eurasian surface wave tomography: group velocities. J. Geophys. Res. 103, 4839–4878.

Ritzwoller, M.H., Shapiro, N.M., Barmin, M.P., Levshin, A.L., 2002. Global surface wave diffraction tomography. J. Geophys. Res. 107(B12), 2335, doi:10.1029/2002JB001777.

San'kov, A.V., Levi, K.G., Calais, E., Déverchère, J., Lesne, O., Lukhnev, A.V., Miroshnichenko, A.I., Buddo, V.Yu., Zalutsky, V.T., Bashkuev, Yu.B., 1999. Historic and Holocene horizontal movements measured at the Baikal geodynamic test ground. Geologiya i Geofizika (Russian Geology and Geophysics) 40 (3), 422–430 (414–421).

Tychkov, S.A., Rychkova, E.V., Vasilevskii, A.N., 1998. Interaction between a plume and thermal convection in the continental upper mantle. Geologiya i Geofizika (Russian Geology and Geophysics) 39 (4), 419–431 (423–434).

Tychkov, S.A., Vasilevskii, A.N., Rychkova, E.V., 1999. Plume evolution beneath continental lithosphere of variable thickness. Geologiya i Geofizika (Russian Geology and Geophysics) 40 (8), 1182–1196 (1163–1176).

Vergnolle, M., Pollitz, F., Calais, E., 2003. Constraints on the viscosity of the continental crust and mantle from GPS measurements and postseismic deformation models in western Mongolia. J. Geophys. Res. 108 (B10), 2502, doi:10.1029/2002JB002374.

Villasenor, A., Ritzwoller, M.H., Levshin, A.L., Barmin, M.P., Engdahl, E.R., Spakman, W., Trampert, J., 2001. Shear velocity structure of central Eurasia from inversion of surface wave velocities. Phys. Earth Planet. Inter. 123, 169–184.

Wu, F.T., Levshin, A., 1994. Surface-wave group velocity tomography of East Asia. Phys. Earth Planet. Inter. 84, 59–77.

Wu, F.T., Levshin, A.L., Kozhevnikov, V.M., 1997. Rayleigh-wave group velocity tomography of Siberia, China and the vicinity. Pure Appl. Geophys. 149, 447–473.

Yakovlev, A.V., Koulakov, I.Yu., Tychkov, S.A., 2007. Moho depths and three-dimensional velocity structure of the crust and upper mantle beneath the Baikal region, from local tomography. Russian Geology and Geophysics (Geologiya i Geofizika) 48 (2), 204–220 (261–282).

Yanovskaya, T.B., Kozhevnikov, V.M., 2000. 3D S-wave velocity pattern in the upper mantle beneath the continent of Asia from Rayleigh wave data. Phys. Earth Planet. Inter. 138, 263–278.

Yarmolyuk, V.V., Kovalenko, V.I., 2003. Deep geodynamics and mantle plumes: Implications for the origin of the Central Asian foldbelt. Petrologiya 11 (6), 504–531.

Yarmolyuk, V.V., Kovalenko, V.I., Bogatikov, O.A., 1990. The South Baikal mantle hotspot and its role in the origin of the Baikal rift zone. Dokl. Akad. Nauk SSSR 312 (1), 187–191.

Yarmolyuk, V.V., Kovalenko, V.I., Ivanov, V.G., 1995. Late Mesozoic-Cenozoic within-plate volcanic province of Central and Eastern Asia: The projection of a mantle hot field. Geotektonika 5, 41–67.

Zorin, Y., Cordell, L., 1991. Crustal extension in the Baikal rift zone. Tectonophysics 198, 117–121.

Zorin, Y.A., Turutanov, E.Kh., Mordvinova, V.V., Kozhevnikov, V.M., Yanovskaya, T.B., Treussov, A.V., 2003. The Baikal rift zone: the effect of mantle plumes on older structure. Tectonophysics 271, 153–173.

Zorin, Yu.A., Turutanov, E.Kh., 2005. Plumes and geodynamics of the Baikal rift zone. Russian Geology and Geophysics (Geologiya i Geofizika) 46 (7), 685–699 (669–682).

Editorial responsibility: N.L. Dobretsov
18 July 2007